The effects of surface roughness geometry of flow undergoing Poiseuille flow by molecular dynamics simulation

H. Noorian · D. Toghraie · A. R. Azimian

Abstract Numerical simulation of Poiseuille flow of liquid Argon in a rough nano-channel using the non-equilibrium molecular dynamics simulation is performed. Density and velocity profiles across the channel are investigated in which roughness is implemented only on the lower wall. The Lennard–Jones potential is used to model the interactions between all particles. The effects of surface roughness geometry, gap between roughness elements (or roughness periodicity), surface roughness height and surface attraction energy on the behavior of the flow undergoing Poiseuille flow are presented. Results show that surface shape and roughness height have a decisive role on the flow behaviors. In fact, by increasing the roughness ratio (height to base ratio), the slip velocity and the maximum velocity in the channel cross section are reduced, and the density fluctuations near the wall increases. Results also show that the maximum density near the wall for a rough surface is less than a smooth wall. Moreover, the simulation results show that the effect of triangle roughness surface on the flow behavior is more than the cylindrical ones.

List of symbols

AR	Roughness aspect ratio
d	Ratio of height to base surface roughness

H. Noorian
Department of Mechanical Engineering, Isfahan University of Technology, Isfahan, Iran
e-mail: hamzehnorian@gmail.com

D. Toghraie (✉) · A. R. Azimian
Department of Mechanical Engineering, Islamic Azad University, Khomeinishahr Branch, Isfahan, Iran
e-mail: Toghraee@iaukhsh.ac.ir

A. R. Azimian
e-mail: Azimian@cc.iut.ac.ir

$AR = h/L$	Roughness aspect ratio
$\vec{F}_{ext}$	External force (N)
h	Roughness height
H	Channel height
N_{atm}	Number of atoms (non-dimensional)
r	Position vector (m)
r_{ij}	Inter-particle separation (m)
T	Temperature (K)
T_{wall}	Wall temperature
v	Velocity vector (m s^{-1})
z	Height (m)

Greek symbols

|	
$\vec{\nabla}$	Dell gradient
σ	Length parameter of argon (m)
ρ	Density (kg m^{-3})
ε	Energy parameter (J)
ε_s	Energy parameter for solid (J)
ϕ	Potential function (J)
ϕ_w	Wall potential function (J)
δt	Time step (s)

Subscripts

c	Cutoff
i	ith
w	Wall
x	x-Direction
y	y-Direction
z	z-Direction

1 Introduction

In fluid flow calculation, there are basically two ways to treat the flow field; the first one is to consider the fluid as a

Table 1 Reduced physical quantities

|	Length (M)	Energy (J)	Mass (kg)	Time (s)	Velocity (m s^{-1})	Force (N)	Pressure (N m^{-2})	Temperature (K)
Unit	σ	ε	m	$\sigma \, (m/\varepsilon)^{1/2}$	$(m/\varepsilon)^{1/2}$	ε/σ	ε/σ^3	ε/k_B
Value for argon	3.4×10^{-10}	1.65×10^{-21}	6.69×10^{-26}	2.17×10^{-12}	1.57×10^{2}	4.85×10^{-12}	4.20×10^{7}	120
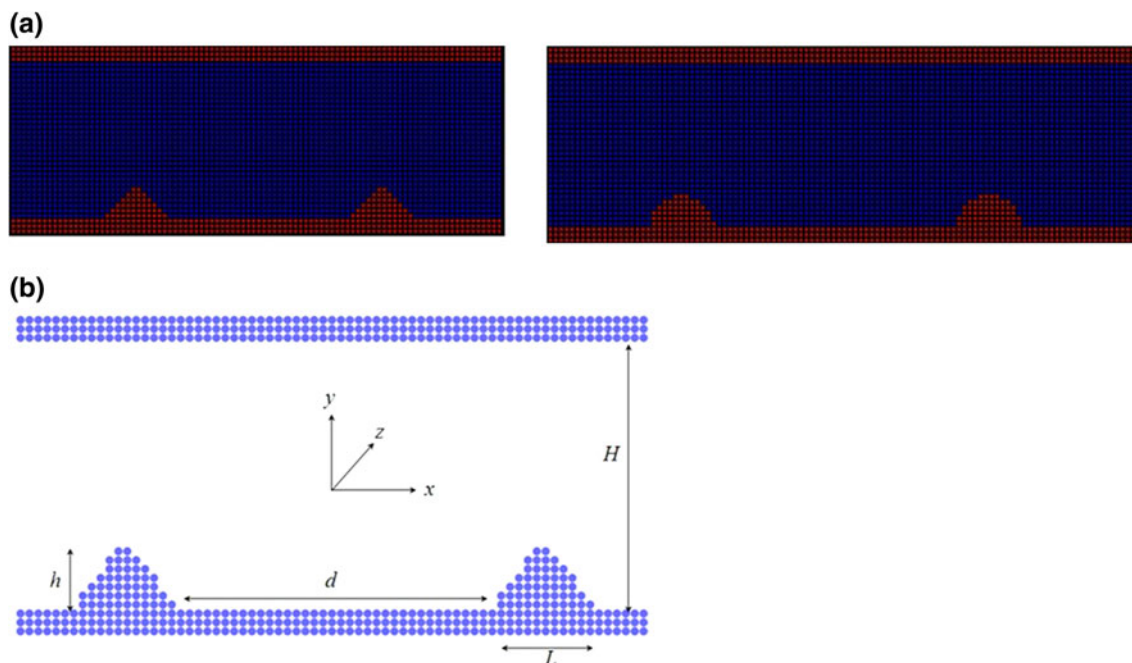
Fig. 1 **a** 2D snapshot of a channel under the presence of nano scale surface roughness. **b** 2D snapshot of a channel under the presence of nano scale surface roughness

number of molecules and in the second case it is considered as a continuum. The first approach is a deterministic approach while in the second approach which is a continuum approach, the velocity, density, pressure, etc. are all defined at every point in the space and time, and the conservation laws lead to Navier–Stokes equations. When the characteristic length of a fluid domain is small, the macroscopic theory is not efficient and may break down. Researchers have dealt with the question whether or not the classical Navier–Stokes equations are valid in channels of small sizes. Observations show that in nanoscale, as the length scale over which the fluid velocity changes approaches the slip length, the fluid can undergo slip at the wall-fluid interface and the usual assumptions of the classical continuum theory with a no-slip boundary condition can break down. From a theoretical point of view, the parameters controlling the degree of slip are still greatly unknown. Previous experimental studies have shown that the boundary slip is highly affected by the solid–fluid interaction energy, the wetting of surface and the surface roughness [1–8]. As experimental observation of flow

behavior near the boundary and interface in a nano scale level is extremely difficult, the numerical simulation based on molecular dynamics offer ideal technique for studying the effects of solid–fluid surface properties on the wall slip phenomena. In practice, few surfaces are smooth in actual nano fluidic systems. As the characteristic length of the surface roughness is in the order of molecular structure, the effects of surface roughness on the rheology and fluid slip become important [9]. Mo and Rosenberger [10] studied a 2-D channel with atomically rough walls. Sinusoidal and randomly roughened walls were used in their simulation. Their results indicated that the Knudsen number alone is not a good criterion for the flow behavior near the wall. The ratio of l/A, should also be used to validate the exact behavior of fluid at solid interface. Where l is the molecular mean free path and A is the amplitude of roughness of surface. Jabbarzadeh and Atkinson [11] indicated that the slip length is strongly influenced by the strength of the liquid/solid interaction potential and the degree of commensurability between the liquid particles and wall atoms. Chang and Maginn [12] studied the phenomena of wall slip

occurring in the rarefied gases flowing through micro- and nano-channels. They showed that how small differences in slip coefficients can be exploited for the kinetic separation of gases. Gala and Attard [13] investigated the effect of atomic roughness on the slip length at fluid–solid interface for a sheared flow. In their model, atomic roughness was simulated by varying the size and spacing between solid atoms at constant packing fraction while the interaction parameters and the thermodynamic state of the fluid were kept constant. Their results indicated that the fluid–solid slip length exhibits nonmonotonic behavior as the solid structure is varied from smooth to rough. Slip occurred for both smooth and rough surfaces while the fluid stick happened only at some surfaces with intermediate values of roughness. Bing Yang and Zeng-Yang [14] studied the rarefied gas flow in a submicron channel in which surface roughness was represented by arrays of triangular modules. They investigated the effects of rarefaction and surface roughness on the boundary conditions and the flow characteristics. Their study showed the decrease of slip as the roughness of the surface increased. They noticed that the friction constant increased while the surface roughness is increased. Ogata et al. [15] simulated formation of molecularly thin liquid bridge between solid surfaces having molecular-scale roughness by using the molecular dynamics. They found that the layered molecular arrangement inside the liquid bridge was disturbed by the molecular-scale roughness on the surfaces and the projected profiles were able to be approximated by arcs. Priezjev [16] used Molecular dynamics simulations to investigate the influence of molecular-scale surface roughness on the slip behavior in thin liquid films. He found that both periodically and randomly corrugated rigid surfaces reduce the slip length and its shear rate dependence. Kunert and Harting [17] performed simulations of pressure driven flow between two rough plates with and without hydrophobic fluid–wall interaction. They showed that for rough surfaces with a hydrophobic fluid–wall interaction, there is a strong nonlinear effect that leads to an increase of the slip length by a factor of three for small interactions. Ziarani and Mohamad [18] studied the rarified gas flow through a 2-D atomically rough micro channel with molecular dynamics simulation. They indicated that even the roughness topology will affect the flow boundaries. Sofos and Karakasidis [19] further revealed the significant roughness effect on the potential energy distribution, fluid atom localization, streaming velocity profiles, and slip length, which indicate that these effects should always be considered in nanoflow designs. Nikolaos and Dimitris [20] simulated the effects of nano scale surface roughness in a channel undergoing Poiseuille flow with MD simulation. Simulation results indicated a nonlinear variation of slip as a factor of roughness amplitude.

Kamali and Kharazmi [21] developed a molecular based scheme for simulating of surface roughness effects on nano- and micro-scale flows. Their simulation results suggested that both the wall fluid interaction and surface roughness are important and should be considered simultaneously in determining the nano-structures and profiles of monatomic fluid flow in a nanochannel. Also, their simulation results showed that the roughness and cavitations of the same dimensions induce different local density patterns while the overall average pattern might be the same. Li et al. [22] reviewed the methods and the applications of MD simulation in liquid flows in nanochannels. They
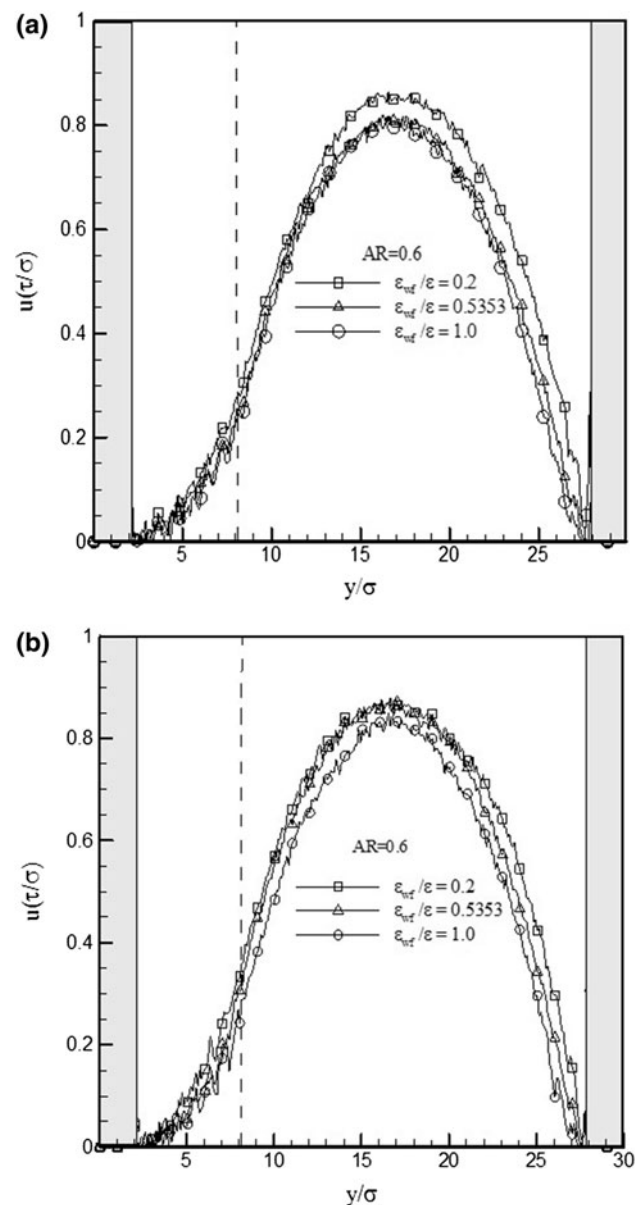
Fig. 2 a Effects of surface attraction energies on the velocity profile in *triangle* geometry. **b** Effects of surface attraction energies on the velocity profile in *cylinder* geometry
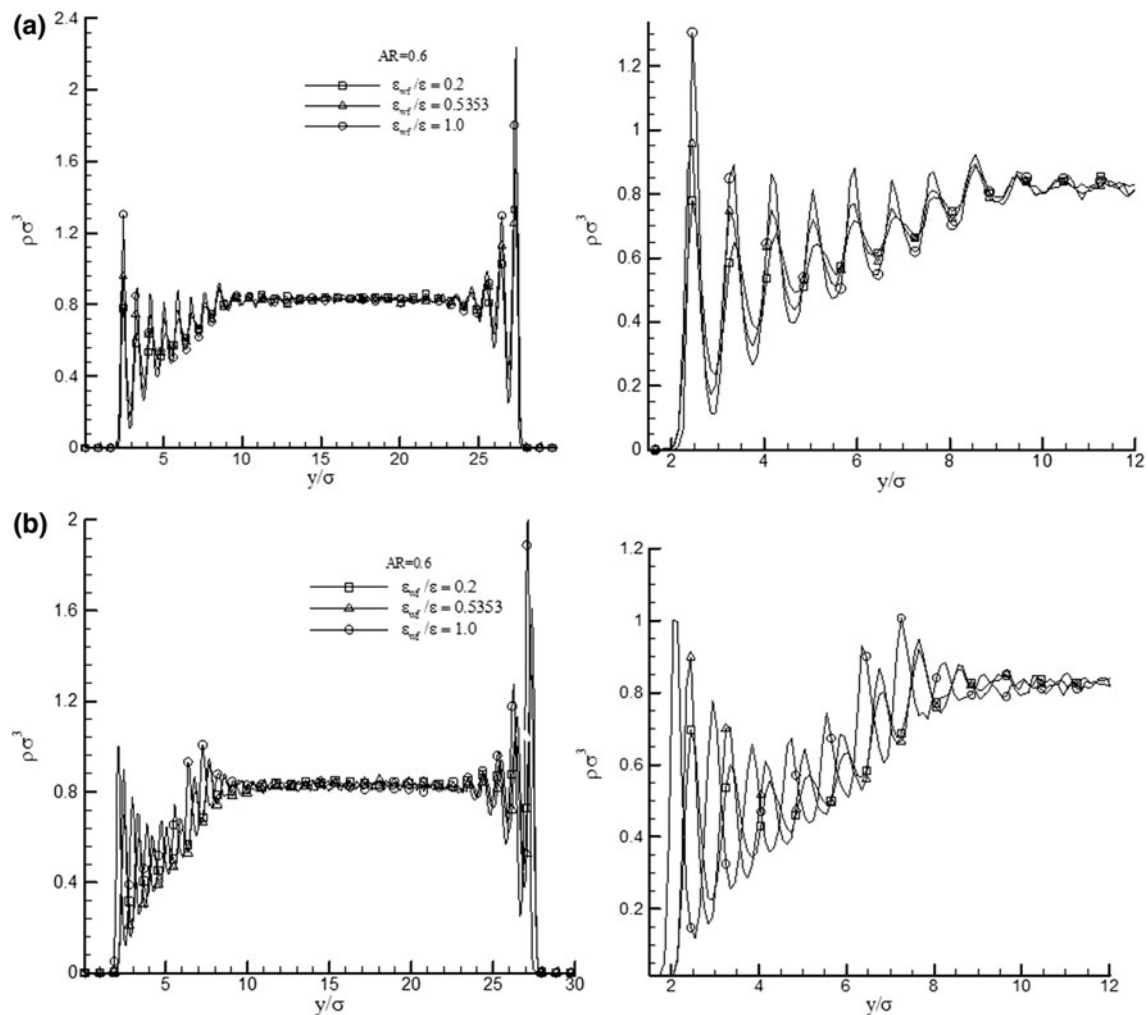
Fig. 3 a Effects of surface attraction energies on the density profile in *triangle* geometry. b Effects of surface attraction energies on the density profile in *cylinder* geometry

focused on the fundamental research and the rationality of the model hypotheses. They summarized the important discoveries in this research field and proposed some worthwhile future research directions. Kamali and Kharazmi [21] examined the surface roughness effects on the fluid flow in a nano channel of simple fluids in hydrophobic and hydrophilic walls by molecular dynamics simulation. Chen et al. [23] conducted a molecular dynamics simulation of slip boundary for fluid flow past a solid surface incorporating roughness effect. Their results indicated that interfacial slip develops if the wall is effectively uncorrugated.

As mentioned earlier, in these articles [1–23], various parameters such as slip length, channel width, surface attraction energy, slip velocity, interface wettability, surface roughness, external force, and heat transfer were studied. From each work different aspects of Poiseuille flow were studied and therefore, different results were

obtained that each work could be useful in its position. However, a lack of a generality in terms of surface roughness geometry, the gap between roughness elements (or roughness periodicity), the surface roughness height and the surface attraction energy were observed. Therefore, it seems that this work can make a good contribution to the removal of shortcomings in other works. Hence, the objective of this paper is to examine the effect of these parameters in order to understand the fluid flow behavior in the rough nano channels. The NEMD simulations of simple Lennard–Jones fluids subject to an inlet driving force in a nanochannel were carried out. Also a planer poiseuille flow of liquid argon is studied using molecular dynamics simulation. In the present work, velocity rescaling is used, together with the velocity integrator, for integration of the trajectories of the particles. For this purpose, near the wall region, along the flow-direction, thermostats act on both sides. The interfacial density profiles at different
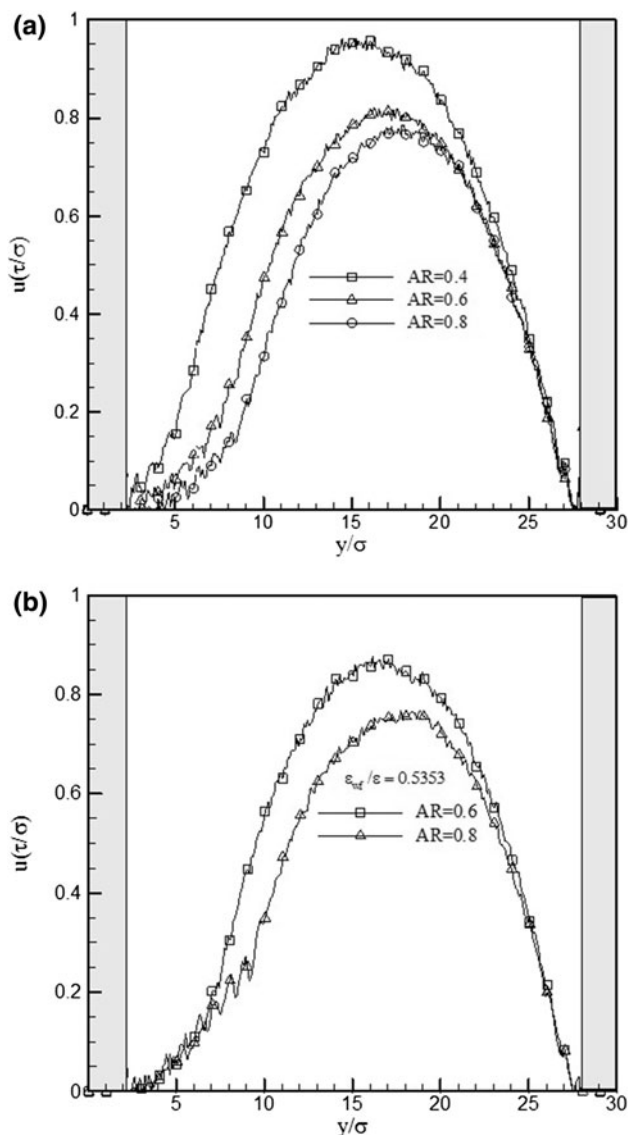
Fig. 4 a Effects of height roughness on the velocity profile in *triangle* geometry. **b** Effects of height roughness on the velocity profile in *cylinder* geometry

magnitudes of the height roughness are obtained. Also, the effect of gap between roughness elements on the velocity profiles is examined.

2 Simulation

In this paper, the large-scale atomic/molecular massively parallel simulation (LAMMPS) were used, which is an available open-source software for molecular dynamics simulation. This program is written in C++ and was developed at Sandia National Labs. LAMMPS is selected for this study due to its simplicity and ease of operation. Dimensionless physical quantities (Lennard–Jones reduced

units) are used for convenience as well as to facilitate scale-up of the system. A simple fluid of argon using Lennard–Jones (12–6) potential as expressed in single atom situation is considered:

$$\phi(r_{ij}) = \left\{ 4\varepsilon \left[\left(\frac{\sigma}{r_{ij}} \right)^{12} - \left(\frac{\sigma}{r_{ij}} \right)^{6} \right] \right\} \tag{1}$$

where $\phi(r_{ij})$ is the interaction potential between two particles, ε is the depth of the potential energy that governs the strength of interaction and σ is the finite distance where the interparticle potential is zero and r_{ij} is the distance between the two particles [24, 25]. Table 1 shows the units used in our argon MD simulation [26] where k is the Boltzmann constant. Here after, all quantities will be given in terms of the Lennard–Jones reduced units. Table 1 shows the units used in MD simulation of particles interacting by the Lennard–Jones potential [26]. The simulation region is cuboids with unit lengths of 40, 25.75 and 5 (molecular units) along x-, y- and z-directions respectively as required in LAMMPS input file. Periodic boundary conditions are applied along x-and z-directions while in y-direction a non-periodic and shrink-wrapped boundary is applied. The shrink-wrapped boundary means that the position of the face is set so as to encompass the atoms in that direction; no matter how far they move [27].

In other words, when a particle enters or leaves the simulation region, an image particle leaves or enters this region, such that the number of particles in the simulation region is always constant [26]. In our simulation, we apply a constant force to each particle along the nanochannel (x-direction). For solid–liquid interactions, the following modified Lennard–Jones potential function is used [28]:

$$\phi_w(r_{ij}) = \left\{ 4\varepsilon_{sf} \left[\left(\frac{\sigma_{sf}}{z} \right)^{12} - \left(\frac{\sigma_{sf}}{z} \right)^{6} \right] \right\} \tag{2}$$

where the Lorenthz–Berthelot mixing rule [29] is applied to the system for calculating σ_{sf} and ε_{sf}

$$\varepsilon_{Sf} = \sqrt{\varepsilon_S \varepsilon_f}, \quad \sigma_{Sf} = \frac{\sigma_S + \sigma_f}{2} \tag{3}$$

When a two-body potential model is chosen, the interaction force between a pair of molecules can be derived from the potential model in such a way that the following relation could be used:

$$\vec{F}_i = \sum_{i \neq j} F_{ij} + \vec{F}_{ext} = m_i \frac{d^2 r_i}{dt^2} + \vec{F}_{ext} = m_i \frac{dv_i}{dt} + \vec{F}_{ext}$$
$$\vec{F}_{ij} = -\vec{\nabla}(\phi + \phi_w) \tag{4}$$

where $\vec{F}_{ext}$ is the inlet external driving force per molecule in the x direction to characterize the forced flow in nanochannels. By integrating Eq. 4, the position vector r_i and
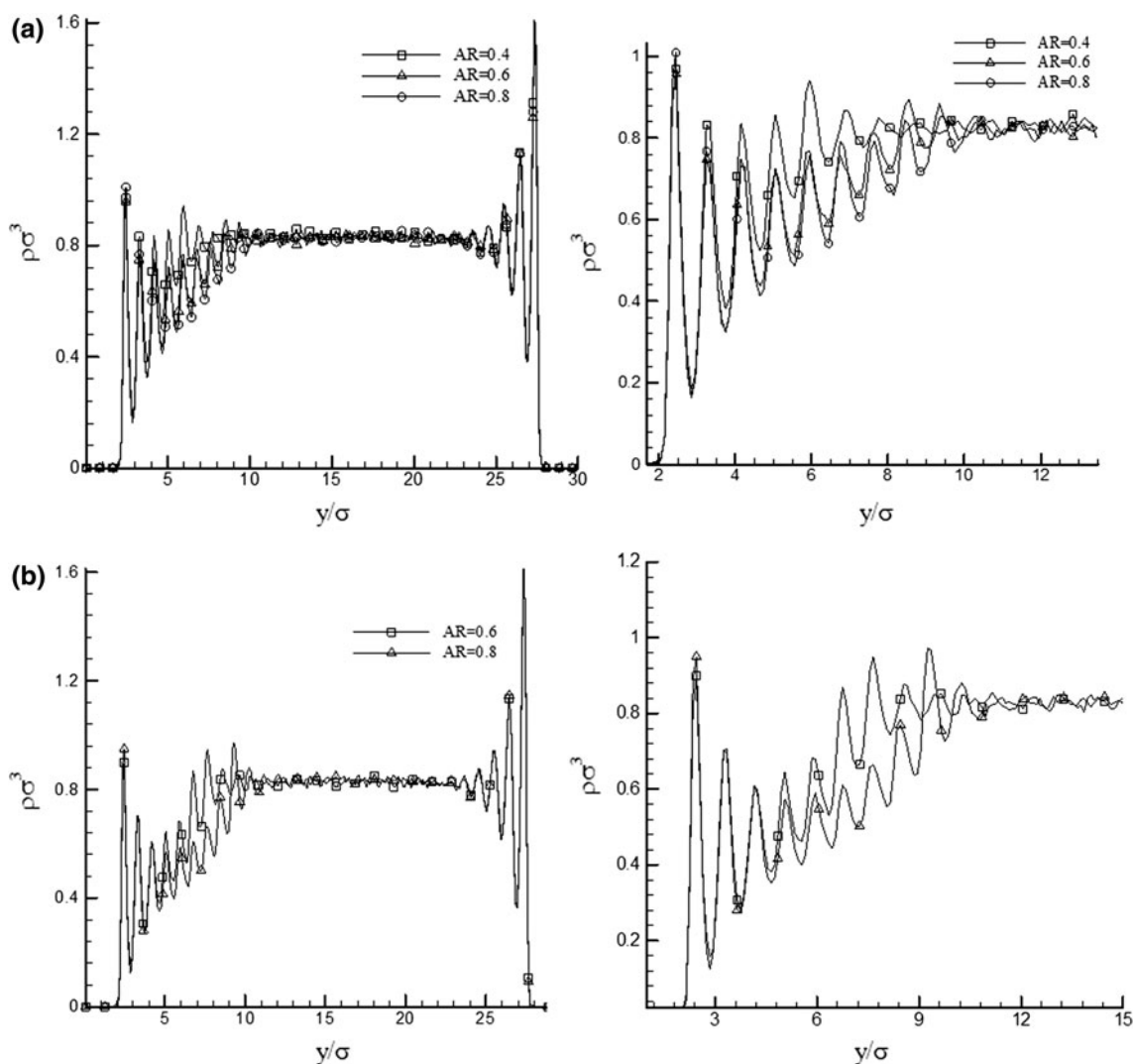
Fig. 5 **a** Effects of height roughness on the density profile in *triangle* geometry. **b** Effects of height roughness on the density profile in *cylinder* geometry


Fig. 6 2D snapshot of gap between *triangle* and *cylinder* roughness elements
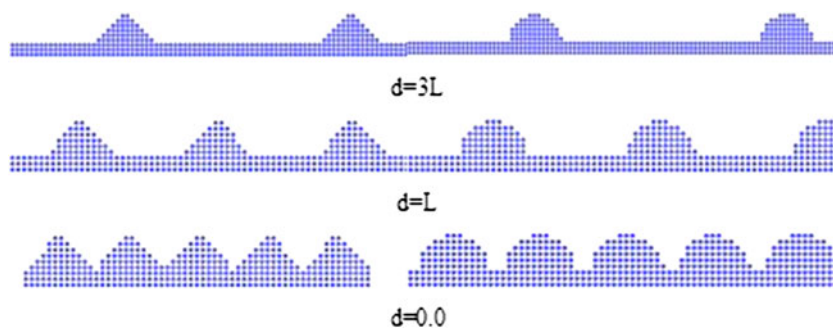
velocity vector v_i could be found and then the thermodynamic properties of simulation domain can be calculated using r_i and v_i. Velocity rescaling is done through a velocity rescaling thermostat by LAMMPS which this thermostat is being used in all simulations in this paper to control the temperature. For velocity rescaling the velocities are first updated from the forces acting on the particles and then rescaled at each time step.

Since the total kinetic energy of the system fluctuates, the instantaneous temperature is defined as a fluctuating
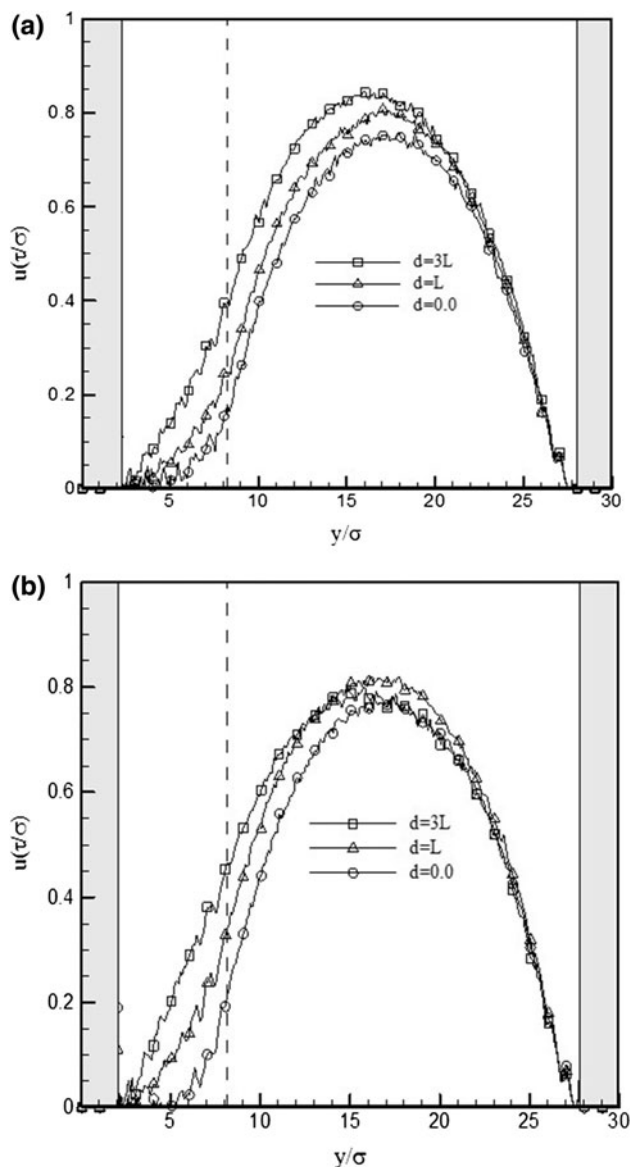
Fig. 7 a Gap between roughness elements d on the velocity profile in *triangle* geometry. **b** Gap between roughness elements d on the velocity profile in *cylinder* geometry

kinetic energy per particle at each slab, per degree of freedom.

It is obvious that a good intermolecular dynamics program needs a good algorithm to integrate the Newton's equation of motion. The integration of the equation of motion is straightforward. Velocity Verlet method [30] is used for integration of the Newton's equation.

The advantage of this algorithm is that the calculations of velocities are in phase with the positions. The initial condition for each molecule is usually assigned by using the Gaussian distribution based on the specified temperature.

The system reaches to equilibrium state after 500,000 time steps and then NEMD simulations are applied. In all

simulation cases, more than 2,000,000 time steps were used for data sampling. The fluid is confined to flow between two solid planar walls parallel to xz plane as shown in Fig. 1a, b.

Each wall consists of atoms forming two [100] planes of an FCC crystal and each atom have a mass of 1. The upper solid surface is smooth while the bottom wall is decorated with roughness with variable height as shown in Fig. 1. It should be noted that any argon atom within the simulation region have interactions with neighboring fluid and wall atoms. The applied force on the fluid atoms is specified to be $0.05 \ \varepsilon\sigma^{-1}$ in the x-direction with constant temperature of $1.1 \ \varepsilon k_B^{-1}$. In this study the numerical experiments were carried out for the gap between roughness elements, roughness aspect ratio and attraction energy varying from $d = 3L$ to $d = 0.0$, $AR = 0.4$–0.8σ and $\varepsilon_{sf} = 0.2\varepsilon$ to $\varepsilon_{sf} = 0.2\varepsilon$.

3 Results and discussion

In any velocity profile, the colored panes represent the solid surface of the nanochannels and the vertical dashed lines show the height of surface roughness. Figure 2 shows the effects of the surface attraction energy on the velocity profile under the presence of roughness with both triangular and cylindrical roughness elements. As shown the fluid particles velocity near the rough wall in both cases tends to a zero value. This is due to the trapping of fluid particles between the roughness elements. Therefore, slip velocity and the maximum flow velocity decreases, which is due to the surface attraction energies. Figure 3 shows the average density profiles under various wall-fluid interaction parameters. As shown in both rough cases, the density fluctuation amplitude increases as surface attraction energy increases. Comparison of the surface roughness in $y/\sigma = 6.25$ with that of $y/\sigma = 2.25$, shows that the density value in $y/\sigma = 6.25$ is lower that of $y/\sigma = 2.25$. This is due to the reduction of surface effects. Figure 4 shows the effect of roughness height on the velocity profiles in both rough cases. As shown the slip velocity and the maximum flow velocity decrease while the roughness height increases. Furthermore, by trapping more particles inside the roughness elements the thickness of the fluid layers will increase. The fluid velocity in this layer is zero. Moreover, the distance that the velocity profile is deviated is equal to the roughness height. Figure 5 shows the fluid velocity profiles under various surface roughness heights in both rough cases. As shown by increasing the surface roughness height, the wall effects penetrate to a greater depth in the fluid inside the channel.

Figure 6 shows a 2D snapshot of the gap between the triangular and the cylindrical roughness elements, where d
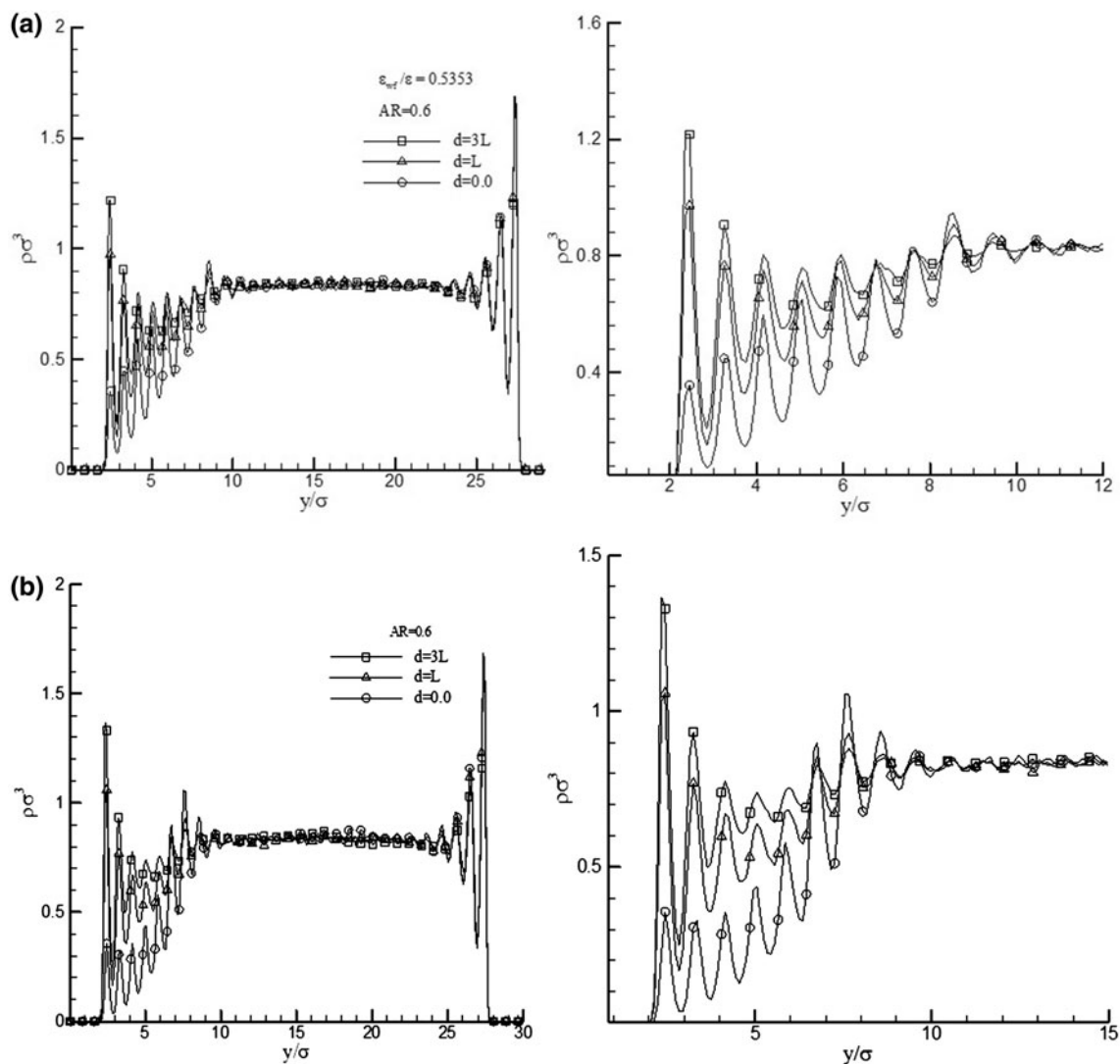
Fig. 8 a Effects gap between roughness elements on the density profile in *triangle* geometry. b Effects gap between roughness elements on the density profile in *cylinder* geometry

is gap between roughness elements and L is the base length of the surface roughness. Figure 7 shows that by increasing the number of roughness elements in a unit length in cases (decrease of gap between roughness elements, which have been shown in Fig. 6), the maximum velocity, and the slip velocity will decrees. This is due to the fact that by reducing the gap between the roughness elements; the numbers of particles which are trapped between the roughness elements have lower freedom. Therefore, their velocity will be equal to wall velocity. Figure 8 shows that, in both roughness geometries, when the gap between roughness elements is equal to zero, the first layer of fluid has the lowest density. It also shows that by moving away further from the wall surface the fluid layers become denser. Eventually they converge to the fluid density in $y/\sigma = 8.25$. This is due to the fact that,

the fluid particles near the rough wall surface, are influenced by stronger repulsion force, and therefore, the particles density near the surface becomes less than that of the other layers of the fluid. Going away further from the channel surface, the gap between the roughness elements increases, therefore, the repulsion force between particles is reduced, and the fluid density increases. When the gap between the roughness elements is 3L, the layer of the fluid has the highest density. This is due to the fact that the reduced repulsive forces between particles which are due to the increase of the gap between roughness elements, causes the density of the first layer of fluid near the wall to decrease. Moreover, the increased gap between the roughness elements decreases the amplitude of the density fluctuations. This is due to the fact that in this case the particles can move more freely.
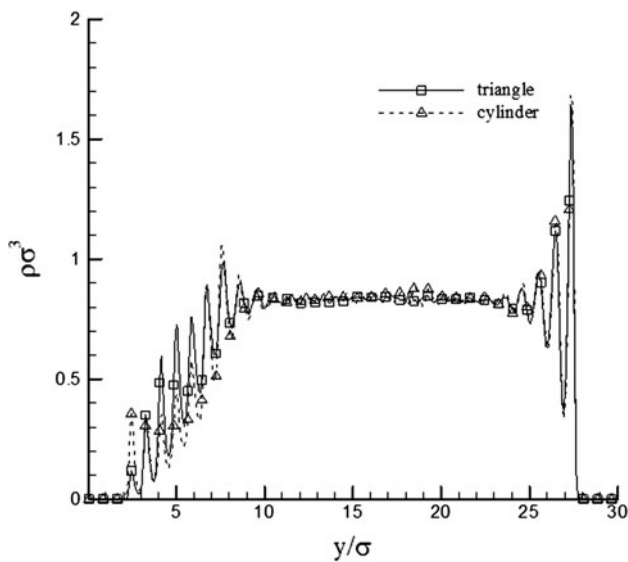
Fig. 9 Comparison density profile in *cylindrical* and *triangular* surface roughness
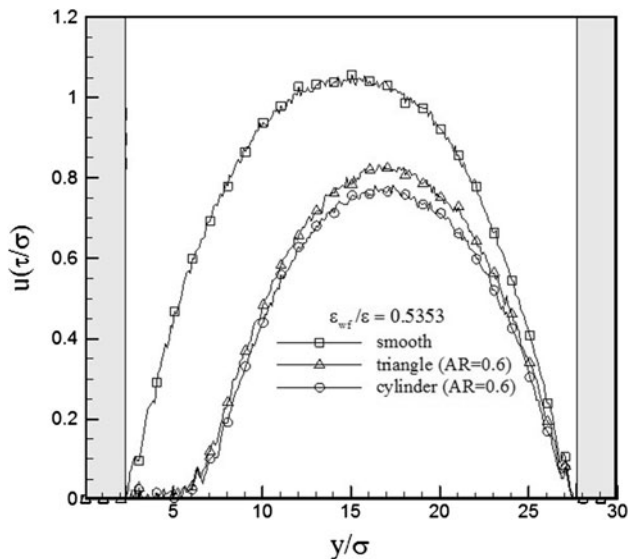
Fig. 10 Velocity profile for cylindrical and triangular roughness surface in comparison with smooth channels

According to Fig. 7 although by increasing the depth of energy and the velocity decreases, the changes in the ratio of energy depth on the velocity are insignificant. This is due to the fact that the increase in depth of energy causes more particles of the fluid to trap between the roughness elements. This, furthermore, leads to an increase in repulsive force between particles. Hence, the fluid particles are affected by both the interaction forces between fluid particles and wall, and the repulsion force between particles. This is the reason why, for high roughness ratios, the effect of interaction force decreases.

3.1 Comparison of a rough surface with cylindrical and triangular roughness elements with a flat channel

Here two roughness geometries are compared with a case that the distance d within roughness elements is zero. According to Fig. 9 the amplitude of the fluctuations near the wall for cylindrical roughness elements is more than that of triangular elements which is a sign of fluid particles trapping between the cylindrical elements. As Fig. 10 shows the maximum velocity in a surface with triangular roughness elements is more than that of a surface with cylindrical roughness elements. This shows that the cylindrical surface roughness affects the flow velocity more than the triangular geometry. This is to the fact that the number of particles that are trapped between cylindrical roughness elements is more than that of triangular elements. Therefore, more fluid particles will have near zero velocities.

4 Conclusions

In this study, the non-equilibrium molecular dynamics simulation of Poiseuille flow of liquid argon in a rough nanochannel is presented. The effects of triangular and cylindrical surface roughness elements under various conditions were studied. These conditions include the surface roughness height, the gap between roughness elements and the surface attraction energy. A summary of some important results obtained as follows:

- By reducing the gap between the roughness elements the maximum velocity and slip velocity decreases.
- The effect of reducing the gap between the roughness elements in a surface with triangular roughness elements is more than that of cylindrical one.
- In comparison with smooth channel, the cylindrical roughness surface has more effect on the flow velocity. This causes more particles to trap between the roughnesses elements near the wall.
- Increasing the roughness height causes the density fluctuation to penetrate more fluid in depth.
- Penetration depth of the density fluctuation into the fluid domain is independent of the type of the roughness elements.

The extension of this paper and our previous works [31–34] affords engineers a good option for nanochannel simulation in one and two phase flows. Also, future studies aimed a elucidating the precise nature of boiling flow and two phase heat transfer would be of considerable interest.

References

1. Pit R, Hervet H, Leger L (2000) Direct experimental evidence of slip in hexadecane: solid interfaces. Phys Rev Lett 85:980–983

2. Zhu Y, Granick S (2001) Rate-dependent slip of Newtonian liquid at smooth surface. Phys Rev Lett 87:096105

3. Craig VSJ, Neto C, Williams DRM (2001) Shear-dependent boundary slip in an aqueous Newtonian liquid. Phys Rev Lett 87:054504

4. Tretheway DC, Meinhart CD (2002) Apparent fluid slip at hydrophobic microchannel walls. Phys Fluids 14:L9–L12

5. Bonaccurso E, Kappl M, Butt HJ (2002) Hydrodynamic force measurements: boundary slip of water on hydrophilic surfaces and electrokinetic effects. Phys Rev Lett 88:076103

6. Cottin-Bizonne C, Charlaix E, Bocquet L, Barrat JL (2003) Low-friction flows of liquid at nanopatterned interfaces. Nat Mater 2:237–240

7. Choi CH, Johan K, Westin A, Breuer KS (2003) Apparent slip flows in hydrophilic and hydrophobic microchannels. Phys Fluids 15:2897–2902

8. Ou J, Perot B, Rothstein JP (2004) Laminar drag reduction in microchannels using ultrahydrophobic surfaces. Phys Fluids 16:4635–4643

9. Richardson S (1973) On the no-slip boundary condition. J Fluid Mech 59:707–719

10. Mo G, Rosenberger F (1990) Molecular dynamics simulation of flow in a two dimensional channel with atomically rough. Phys Rev A 42:4688–4692

11. Jabbarzadeh A, Atkinson JD (2000) Effect of the wall roughness on slip and rheological properties of hexadecane in molecular dynamics simulation of coquette shear flow between two sinusoidal walls. Phys Rev E 61:690–699

12. Chang HC, Maginn EJ (2003) Molecular Simulations of Knudsen wall-slip: effect of wall morphology. Mol Simul 29:697–709

13. Gala TM, Attard F (2004) Molecular dynamics study of the effect of atomic roughness on the slip length at the fluid–solid boundary during shear flow. Langmuir 20:3477–3482

14. Bing Yang C, Zeng-Yang G (2004) Rarefied gas flow in rough microchannels by molecular dynamics simulation. Chin Phys Lett 21:1777–1779

15. Ogata S, Fukuzawa K, Mitsuya Y, Ohshima Y (2005) Molecular dynamics simulation of ultra-thin liquid bridging between surfaces having two-dimensional roughness. Microsyst Technol 11:1146–1153

16. Priezjev NV (2007) Effect of surface roughness on rate-dependent slip in simple fluids. J Chem Phys 127:144708–1447014

17. Kunert C, Harting J (2008) Simulation of fluid flow in hydrophobic rough microchannels. Int J Comput Fluid Dyn 22:475–480

18. Ziarani AS, Mohamad AA (2008) Effect of wall roughness on the slip of fluid in a microchannel. Nanoscale Microscale Thermophys Eng 12:154–169

19. Sofos FD, Karakasidis TE (2009) Effects of wall roughness on flow in nanochannels. Phys Rev E 97:026305

20. Nikolaos A, Dimitris D (2010) Surface roughness effects in micro and nanofluidic devices. J Comput Theor Nanosci 7:1825–1830

21. Kamali R, Kharazmi A (2011) Molecular dynamics simulation of surface roughness effects on nano scale flows. Int J Therm Sci 50:226–232

22. Li Y, Xu J, Li D (2010) Molecular dynamics simulation of nanoscale liquid flows. Microfluid Nanofluid 9:1011–1031

23. Chen Y, Zhang C, Shi M, Peterson GP (2012) Slip boundary for fluid flow at rough solid surfaces. Appl Phys Lett 100:074102

24. Plimpton SJ (1995) Fast parallel algorithms for short-range molecular dynamics. J Comput Phys 117:119–126

25. Lennard-Jones JE (1931) Cohesion. Proc Phys Soc 43:461482

26. Beu TA (2002) Molecular dynamics simulations. University Babes-Bolyai, Cluj-Napoca

27. Plimpton SJ, Crozie P, Thompson A (2003) LAMMPS user manual. Sandia National Laboratories, USA

28. Travis KP, Gubbins KE (2000) Poiseuille flow of Lennard–Jones fluids in narrow slit pores. J Chem Phys 112:19841994

29. Ghosh A, Paredes R, Lundg S (2007) Poiseuille flow in nanochannel, use of different thermostats. In: PARTEC conference

30. Stoddrd SD, Ford PJ (1973) Numerical experiments on the stochastic behavior of a Lennard–Jones gas system. Phys Rev A 8:1504–1510

31. Toghraie Semiromi D, Azimian AR (2010) Molecular dynamics simulation of liquid–vapor phase equilibrium by using the modified Lennard–Jones potential function. Heat Mass Transf 46:287–294

32. Toghraie Semiromi D, Azimian AR (2010) Nanoscale Poiseuille flow and effects of modified Lennard–Jones potential function. Heat Mass Transf 46:791–801

33. Toghraie Semiromi D, Azimian AR (2011) Molecular dynamics simulation of nanodroplets with the modified Lennard–Jones potential function. Heat Mass Transf 47:579–588

34. Toghraie Semiromi D, Azimian AR (2012) Molecular dynamics simulation of annular flow boiling with the modified Lennard–Jones potential function. Heat Mass Transf 48:141–152